Inorg. Chem. **2006**, *45*, 5358–5366

Structurally Complex Cobalt Intermetallics Grown from Liquid Aluminum: $Co_{19}Al_{45}Si_{10-x}$ ($x = 0.13$) and $Co_5Al_{14}Si_2$

Xiuni Wu, Susan Latturner, and Mercouri G. Kanatzidis*

Department of Chemistry, Michigan State University, East Lansing, Michigan 48824

Received December 20, 2005

The cobalt aluminum silicides $Co_{19}Al_{45}Si_{10-x}$ ($x = 0.13$) and $Co_5Al_{14}Si_2$ were synthesized in liquid aluminum and characterized by single-crystal X-ray diffraction. $Co_{19}Al_{45}Si_{10-x}$ ($x = 0.13$) crystallizes in the monoclinic space group *C*2/*c* with lattice parameters $a = 19.991(2)$ Å, $b = 19.143(2)$ Å, $c = 12.8137(15)$ Å, $\beta = 123.583(2)°$. $Co_5Al_{14}Si_2$ adopts the orthorhombic space group *Pnma* with cell parameters $a = 13.8948(19)$ Å, $b = 23.039(3)$ Å, $c = 7.3397(10)$ Å. Both structures are exceptionally complex with the Co_2Si_2 rhombus being a common building motif. The coordination environments of cobalt atoms resemble those of the transition metals in typical quasi-crystal approximants. $Co_5Al_{14}Si_2$ shows oxidation resistance in air up to 1000 °C by forming a dense-packed Al_2O_3 layer on the surface of the crystal.

Introduction

Aluminum matrix alloys are technologically useful materials because of their lightweight, special mechanical strength, high thermal and electrical conductivity, etc.[1] For example, aluminum metal-matrix composites (Al-MMCs) have emerged as a critical class of materials for applications in lightweight automotive structures, forgings for suspensions and drivetrains, as well as aerospace development products.[2] The addition of transition metals and silicon into an Al matrix involves the formation of intermetallic phases which contributes to the desirable properties of these materials such as high strength, high-temperature wear and corrosion-resistant coatings[3] and even thermoelectric energy conversion.[4] Moreover, a large number of quasi-crystal approximants occur in the Al-rich region of the Al−TM (TM = transition metal) and related ternary systems.[5] One well-known example is α-MnAlSi, which is a prototype of approximants presenting Mackay-type clusters.[6] Since the quasi-crystalline phases often are found with a composition similar to those of crystalline approximant phases, the detection of new approximants often helps to find new quasi-crystals and aids in the understanding of the local order of the latter compounds.

The ternary phase diagram of Co−Al−Si system presents several phases such as $Co_3Al_4Si_3$,[7] $Co_3Al_{3-x}Si_{4+x}$, and $Co_2Al_{1+x}Si_{2-x}$.[8] Recently, a few new ternary phases were described by Richter et al., including $Co_4Al_{7+x}Si_{2-x}$, which shows covalently bonded Al/Si 3D framework with fairly ionic interactions with Co.[9,10] Here we present the two members in the Al-rich region, $Co_{19}Al_{45}Si_{10-x}$ ($x = 0.13$) and $Co_5Al_{14}Si_2$, grown from aluminum flux.[11] Both compounds exhibit surprisingly large unit cells and complex structures; $Co_5Al_{14}Si_2$ shows remarkable thermal oxidation resistance in air up to 1000 °C. Herein, we describe the synthesis, crystal structure, thermal stability and magnetic properties of the title compounds. Our results are in agreement with those of Richter et al. Coordination environments of cobalt are complex and bear a resemblance to those of the transition metals in quasi-crystal approximants. $Co_5Al_{14}Si_2$ shows oxidation resistance in air up to 1000 °C by forming a dense-packed Al_2O_3 film on the surface of the crystal.

* To whom correspondence should be addressed. E-mail: kanatzid@cem.msu.edu.

(1) (a) Kevorkijan, V. *Aluminum* **2002**, *78*, 469. (b) Satyanarayana, K. G.; Pillai, R. M.; Pai, B. C. *Trans. Indian Inst. Metals* **2002**, *55*, 115.
(2) (a) Suresh, S.; Mortensen, A.; Needleman, A. *Fundamentals of Metal-Matrix Composite*; Butterworth-Heinemann: Boston, 1993. (b) Ochiai, S. *Mechanical Properties of Metallic Composite*; Marcel Dekker: New York, 1994.
(3) (a) Wang, H. M.; Lu, X. D.; Liu, Y. F.; Duan, G.; Cai, L. X.; Wang, C. M. *Mater. Sci. Forum* **2003**, *426*−*432*, 2551. (b) Chen, J. H.; Costan, E.; van Huis, M. A.; Xu, Q.; Zandbergen, H. W. *Science* **2006**, *312*, 416−419.
(4) Tokita, S.; Amano, T.; Okabayashi, M.; Nishida, I. A. *Proc. Int. Conf. Thermoelectr. Energy Convers.* **1993**, *12*, 197.
(5) Tamura, N. *Philos. Mag. A* **1997**, *76*, 337.
(6) Frank, F. C.; Kasper, J. S. *Acta Crystallogr. A* **1996**, *52*, 125.
(7) Zarechnyuk, O. S.; German, N. V.; Yanson, T. I.; Rykhal, R. M.; Murav'eva, A. A. *Fazovye Ravnovesiya Met. Splavakh* **1981**, 69.
(8) Schmid-Fetzer, R. *Ternary Alloys*; Petzow, G., Effenberg, G., Eds.; VCH Verlag: Weinheim, 1991; Vol. 4.
(9) Richter, K. W.; Prots, Y.; Grin, Yu. *Inorg. Chem.* **2005**, *44*, 4576.
(10) Richter, K. W.; G. Tordesillas Gutiérrez, *Intermetallics* **2005**, *12*, 848.
(11) Kanatzidis, M. G.; Pöttgen, R.; Jeitschko, W. *Angew. Chem., Int. Ed.* **2005**, *44*, 6996.

10.1021/ic052165k CCC: $33.50
Published on Web 06/14/2006

Table 1. Selected Crystal Structure Data and Refinement[a] Details for $Co_{19}Al_{45}Si_{10-x}$ ($x = 0.13$) and $Co_5Al_{14}Si_2$

empirical formula	$Co_{19}Al_{45}Si_{10-x}$ ($x = 0.13$)	$Co_5Al_{14}Si_2$
formula weight	2614.67	728.55
cryst syst	monoclinic	orthorhombic
space group	*C*2/*c* (no. 15)	*Pnma* (no. 62)
unit cell dimensions	$a = 19.991(2)$ Å	$a = 13.8948(19)$ Å
	$b = 19.143(2)$ Å	$b = 23.039(3)$ Å
	$c = 12.8137(15)$ Å	$c = 7.3397(10)$ Å
	$\beta = 123.583(2)°$	
volume	4085.1(8) Å^3	2349.6(6) Å^3
Z	4	8
density (calculated)	4.251 Mg/m^3	4.119 Mg/m^3
absorption coefficient	8.773 mm^{-1}	8.130 mm^{-1}
F(000)	4952	2760
cryst size	0.23 × 0.13 × 0.09 mm^3	0.22 × 0.18 × 0.26 mm^3
θ range for data collection	1.62−28.10°	1.77−28.14°
reflns collected	21 558	24 268
independent reflns	4644 [*R*(int) = 0.0429]	2789 [*R*(int) = 0.0328]
completeness to $\theta = 28.10°$	92.9%	94.7%
data/restraints/params	4644/0/338	2789/0/199
GOF on F^2	1.030	1.066
final *R* indices [$I > 2\sigma(I)$][b]	R1 = 0.0326, wR2 = 0.0705	R1 = 0.0268, wR2 = 0.0640
R indices (all data)	R1 = 0.0446, wR2 = 0.0746	R1 = 0.0316, wR2 = 0.0686
Largest diff. peak and hole	1.588 and −0.979 e.Å^{-3}	3.007 and −1.111 e.Å^{-3}

[a] Refinement method: full-matrix least-squares on F^2. [b] $R1 = \sum(|F_o| - |F_c|)/\sum|F_o|$; $wR2 = [\sum[w(F_o^2 - F_c^2]/[\sum(w|F_o|^2)^2]^{1/2}$.

Experimental Section

Reagents. The following reagents were used as obtained without further purification: cobalt (−325 mesh, Cerac, 99.9%), vanadium (−325 mesh, Cerac, 99.7%), aluminum pellets (Cerac, 99.99%), and silicon (−325 mesh amorphous powder, Cerac, 99.999%).

Synthesis. $Co_{19}Al_{45}Si_{10-x}$ ($x = 0.13$). In a nitrogen-filled glovebox, 1 mmol of vanadium (0.051 g), 2 mmol of cobalt (0.118 g), 10 mmol of aluminum (0.270 g), and 5 mmol silicon (0.14 g) were combined in an alumina crucible. The crucible was put into a silica tube, which was sealed under the vacuum of 10^{-4} Torr. The sample was then heated to 1000 °C in 15 h, maintained at this temperature for 5 h, and cooled to 850 °C in 2 h. It was annealed at 850 °C for 3 days, cooled to 200 °C in 36 h, and finally cooled to 50 °C in 2 h.

$Co_5Al_{14}Si_2$. In a nitrogen-filled glovebox, 3 mmol of cobalt (0.177 g), 15 mmol of aluminum (0.405 g), and 5 mmol of silicon (0.14 g) were combined in an alumina crucible. The crucible was put into a silica tube, which was sealed under the vacuum of 10^{-4} Torr. The sample was then heated to 1000 °C in 15 h, maintained at this temperature for 5 h, and cooled to 850 °C in 2 h. It stayed at 850 °C for 3 days, cooled to 200 °C in 36 h, and finally cooled to 50 °C in 2 h.

Isolation. The excess aluminum was removed by soaking the crucible in aqueous 5 M NaOH solution overnight. The resulting crystalline product was rinsed with water and dried with acetone. The yield for $Co_{19}Al_{45}Si_{10-x}$ ($x = 0.13$) was ~70% based on the initial amount of cobalt used. $Co_5Al_{14}Si_2$ was obtained as a pure phase with a yield of 90%. Single crystals were selected for elemental analysis, X-ray diffraction, thermal gravimetric analysis, and magnetic measurements. When we tried to produce the phase $Co_{19}Al_{45}Si_{10-x}$ ($x = 0.13$) by direct combination of the elements with arc-melting in the stoichiometric ratio 1.9:4.5:1.0, the phase $Co_5Al_{14}Si_2$ formed instead. Arc−melting reactions were run under Ar atmosphere on a water-cooled copper plate, and the pellets were flipped and remelted three times to ensure a homogeneous distribution of the reactants.

Table 2. Atomic Coordinates ($\times 10^4$) and Equivalent Isotropic Displacement Parameters (Å^2, $\times 10^3$) for $Co_{19}Al_{45}Si_{10-x}$ ($x = 0.13$)[a]

	Wyckoff site	*x*	*y*	*z*	$U_{(eq)}$[b]
Co(1)	8f	752(1)	4023(1)	5417(1)	7(1)
Co(2)	8f	1790(1)	5896(1)	8002(1)	6(1)
Co(3)	8f	6144(1)	9017(1)	9009(1)	5(1)
Co(4)	8f	3150(1)	7111(1)	6806(1)	7(1)
Co(5)	8f	3158(1)	4800(1)	6845(1)	8(1)
Co(6)	8f	4223(1)	5238(1)	9509(1)	8(1)
Co(7)	8f	4343(1)	2922(1)	9487(1)	10(1)
Co(8)	4e	5000	5969(1)	7500	7(1)
Co(9)	8f	1374(1)	7814(1)	9263(1)	5(1)
Co(10)	8f	3327(1)	4063(1)	8855(1)	10(1)
Al(1)	8f	2163(1)	7874(1)	6744(1)	7(1)
Al(2)	8f	4651(1)	7124(1)	8210(1)	8(1)
Al(3)	8f	−300(1)	4113(1)	3249(1)	7(1)
Al(4)	8f	2204(1)	3966(1)	6668(1)	6(1)
Al(5)	8f	1290(1)	7129(1)	7360(1)	8(1)
Al(6)	8f	1244(1)	3321(1)	7368(1)	8(1)
Al(7)	8f	2892(1)	6026(1)	10162(1)	9(1)
Al(8)	8f	3833(1)	6653(1)	5789(1)	7(1)
Al(9)	8f	2937(1)	6781(1)	8451(1)	8(1)
Al(10)	8f	3816(1)	5201(1)	5826(1)	8(1)
Al(11)	8f	4659(1)	4812(1)	8210(1)	7(1)
Al(12)	8f	1190(1)	3510(1)	4091(1)	8(1)
Al(13)	8f	1209(1)	4736(1)	7299(1)	8(1)
Al(14)	8f	4453(1)	6320(1)	10624(1)	13(1)
Al(15)	8f	1705(1)	4804(1)	4757(1)	15(1)
Al(16)	8f	-473(1)	3295(1)	5210(1)	10(1)
Al(17)	8f	3877(1)	3600(1)	7569(1)	9(1)
Al(18)	8f	6860(1)	7887(1)	9747(1)	16(1)
Al(19)	8f	477(1)	5325(1)	4826(1)	10(1)
Al(20)	4e	0	7681(1)	7500	16(1)
Al(21)	8f	2047(1)	6031(1)	6316(1)	12(1)
Al(22)	8f	619(1)	2684(1)	5059(1)	13(1)
Al(23)	8f	3722(1)	5964(1)	7587(1)	7(1)
Si(1)	8f	7485(1)	9093(1)	9607(2)	25(1)[c]
Si(2)	4e	5000	8339(1)	7500	6(1)
Si(3)	8f	2516(1)	7828(1)	9157(1)	6(1)
Si(4)	4e	5000	9678(1)	7500	6(1)
Si(5)	8f	2814(1)	5184(1)	8259(1)	8(1)
Si(6)	8f	5249(1)	5928(1)	9655(1)	7(1)

[a] Estimated standard deviations are in parentheses. [b] $U_{(eq)}$ is defined as one-third of the trace of the orthogonalized U_{ij} tensor. [c] The thermal displacement parameter is large for this site which is only partially occupied. When we refine the structure with mixed occupation of Al and Si, the *R* values and thermal parameters remained at the same level. More importantly, the bond distances between Si(1) and the neighboring Co atoms range from 2.3498(15) to 2.3572(16) Å, which are comparable to the other Si−Co distances. They are much shorter than typical of Al−Co bond distances, which tend to be longer than 2.45 Å.

Table 3. Selected Bond Lengths for $Co_{19}Al_{45}Si_{10-x}$ ($x = 0.13$)

bond	length, Å	bond	length, Å
Co(3)−Si(1)	2.3498(16)	Al(5)−Co(7)	2.4880(13)
Co(3)−Al(6)	2.5884(13)	Al(5)−Al(17)	2.8434(17)
Co(5)−Al(11)	2.5013(14)	Si(2)−Si(4)	2.562(2)
Co(5)−Co(6)	2.9744(8)	Si(3)−Co(9)	2.3587(12)
Al(2)−Al(23)	2.7160(17)	Si(3)−Al(7)	2.6517(17)
Al(2)−Si(6)	2.7666(17)	Si(4)−Co(3)	2.3825(10)

Elemental Analysis. Selected crystals were fixed on the SEM plate using carbon tape. Chemical composition of the products was determined by energy dispersive spectroscopy (EDS) performed on a JEOL JSM-35C scanning electron microscope (SEM) equipped with NORAN EDS detector. Data were acquired by applying a 25 kV accelerating voltage with an accumulation time of 30 s. The atomic ratio in the compounds $Co_{19}Al_{45}Si_{10-x}$ ($x = 0.13$) and $Co_5Al_{14}Si_2$ were determined to be 18.4:41.5:10 (Co/Al/Si) and 5.27:13.6:2 (Co/Al/Si), respectively, in good agreement with the results derived from the single-crystal X-ray analysis.

Table 4. Atomic Coordinates ($\times 10^4$) and Equivalent Isotropic Displacement Parameters (Å^2, $\times 10^3$) for $Co_5Al_{14}Si_2$[a]

	Wyckoff site	x	y	z	$U_{(eq)}$[b]
Co(1)	8d	7853(1)	3393(1)	956(1)	8(1)
Co(2)	8d	5213(1)	6648(1)	1010(1)	8(1)
Co(3)	8d	4393(1)	5755(1)	5767(1)	5(1)
Co(4)	8d	6560(1)	5021(1)	−918(1)	8(1)
Co(5)	4c	5460(1)	2500	3877	8(1)
Co(6)	4c	7092(1)	2500	6132	12(1)
Si(1)	4c	8753(1)	2500	1136(2)	9(1)
Si(2)	8d	4360(1)	4720(1)	5850(1)	7(1)
Si(3)	4c	4769(1)	7500	2858(2)	15(1)
Al(1)	4c	6942(1)	2500	2206(2)	10(1)
Al(2)	8d	6201(1)	5796(1)	1113(2)	6(1)
Al(3)	8d	7672(1)	4218(1)	−968(1)	6(1)
Al(4)	8d	4352(1)	5818(1)	2223(2)	8(1)
Al(5)	8d	2984(1)	5256(1)	4086(2)	9(1)
Al(6)	4c	5110(1)	7500	−778(2)	5(1)
Al(7)	8d	8365(1)	3134(1)	4048(2)	10(1)
Al(8)	8d	4655(1)	5307(1)	8726(2)	11(1)
Al(9)	8d	9607(1)	3415(1)	−287(2)	12(1)
Al(10)	8d	6523(1)	3104(1)	1052(2)	8(1)
Al(11)	8d	8225(1)	3133(1)	−2400(2)	14(1)
Al(12)	8d	4395(1)	6352(1)	−1920(2)	13(1)
Al(13)	8d	3495(1)	6616(1)	4896(2)	17(1)
Al(14)	8d	8918(1)	4173(1)	2089(2)	11(1)
Al(15)	8d	2900(1)	5708(1)	7494(2)	16(1)

[a] Estimated standard deviations are in parentheses. [b] $U_{(eq)}$ is defined as one-third of the trace of the orthogonalized U_{ij} tensor.

Table 5. Selected Bond Lengths for $Co_5Al_{14}Si_2$

bond	length, Å	bond	length, Å
Co(1)−Al(7)	2.4518(12)	Si(1)−Al(9)	2.6347(15)
Co(2)−Al(11)	2.5148(13)	Si(2)−Al(14)	2.5721(16)
Co(3)−Si(2)	2.3686(11)	Si(3)−Co(6)	2.6895(19)
Co(4)−Al(14)	2.4538(12)	Al(1)−Al(12)	2.9093(16)
Co(5)−Si(1)	2.3715(16)	Al(3)−Si(2)	2.6162(15)
Co(5)−Co(6)	2.8075(11)	Al(5)−Co(4)	2.4934(12)

X-ray Crystallography. Single-crystal X-ray diffraction data of $Co_{19}Al_{45}Si_{10-x}$ ($x = 0.13$) and $Co_5Al_{14}Si_2$ were collected at room temperature on a Bruker AXS SMART CCD X-ray diffractometer with graphite-monochromatized Mo Kα ($\lambda = 0.71073$ Å) radiation. Data processing was performed with the SAINTPLUS software package.[12] The face-indexing procedure was used to analytically correct for absorption; the empirical absorption correction was applied to the data using the SADABS program.[13] Both structures were solved using direct methods and refined with the SHELXTL package programs.[14] Since Al and Si could not be distinguished directly from the collected X-ray scattering data, the assignment of Al and Si positions were made on the basis of the bond distances. All atomic positions were refined anisotropically. Table 1 shows the crystallographic refinement data for $Co_{19}Al_{45}Si_{10-x}$ ($x = 0.13$) and $Co_5Al_{14}Si_2$. Tables 2, 3, 4, and 5 give fractional atomic positions, equivalent isotropic thermal displacement parameters, and selected bond distances for $Co_{19}Al_{45}Si_{10-x}$ ($x = 0.13$) and $Co_5Al_{14}Si_2$, respectively.

Differential Thermal Analysis. Thermal gravimetric analysis (TGA) was performed on a Shimadzu TGA-50 thermal gravimetric analyzer. The sample was heated to 900 °C at a rate of 10 °C/min under flowing air, held at 900 °C for 10 min, and then cooled to room temperature at the same rate.

Magnetic Measurements. Magnetic susceptibility measurements were conducted on the polycrystalline samples of $Co_{19}Al_{45}Si_{10-x}$ ($x = 0.13$) and $Co_5Al_{14}Si_2$ using a Quantum Design MPMS SQUID magnetometer. EDS-analyzed crystals were ground into powder, which was sealed in Kapton tape and placed into the magnetometer. The data were collected in the temperature range 3−300 K at 1000 G, while field-dependent magnetic measurements, conducted at 5 K, were carried out in fields up to ±5.5 T. The magnetic contribution from Kapton tape was subtracted for correction.

Results and Discussion

Synthesis. $Co_{19}Al_{45}Si_{10-x}$ ($x = 0.13$) was found in an effort to explore the system V−Co−Al−Si using Al as the flux. Vanadium did not incorporate into the product and a new ternary phase $Co_{19}Al_{45}Si_{10-x}$ ($x = 0.13$) formed instead. The yield of the reaction was 70% based on the initial amount of cobalt used. Surprisingly, the side products were mainly unreacted vanadium and recrystallized Si. Several attempts to make this compound with only Co and Si in Al flux or by direct combination with arc-melting were not successful.[15] These attempts resulted in $Co_5Al_{14}Si_2$.

Crystal Structure of $Co_{19}Al_{45}Si_{10-x}$ ($x = 0.13$). $Co_{19}Al_{45}Si_{10-x}$ ($x = 0.13$) crystallizes in the group *C*2/*c*, and its

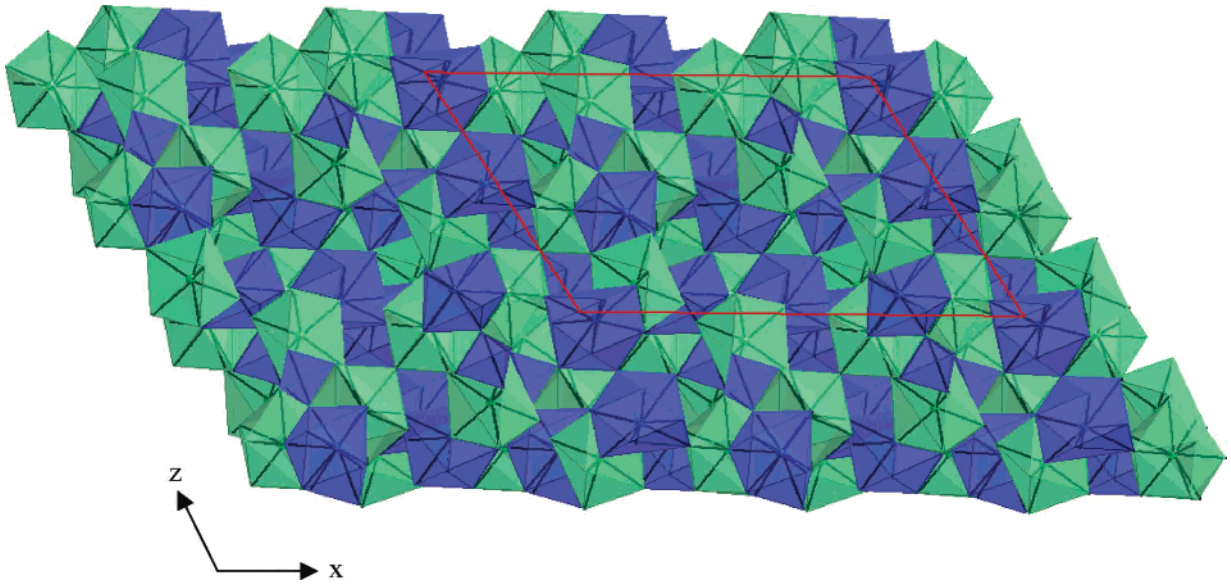

Figure 1. Structure of $Co_{19}Al_{45}Si_{10-x}$ ($x = 0.13$) in polyhedral representation viewed down the *b* axis. Co, green; Si, blue.

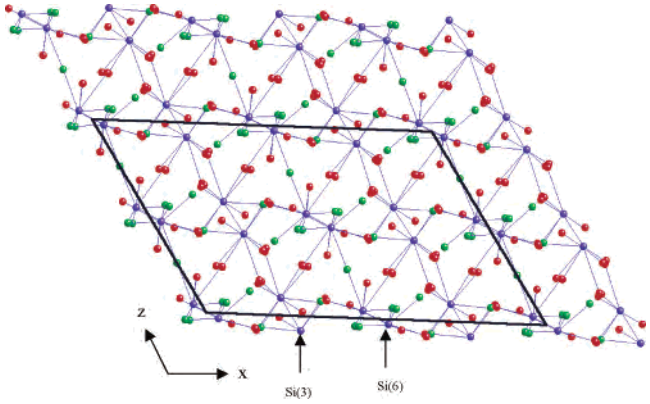

Figure 2. Structure of $Co_{19}Al_{45}Si_{10-x}$ ($x = 0.13$): framework composed of Si(3)- and Si(6)-centered slabs. Co, green; Al, red; Si, blue.

large unit cell contains 10 Co, 23 Al, and 6 Si independent sites with a total of 296 atoms. All the atomic sites are ordered except for Si(1), which is only 92% occupied.

The very high structural complexity presents difficulties in describing this structure in a straightforward fashion. A careful examination reveals that no high-symmetry first-neighbor polyhedron can be found around any atomic site with the exception of perhaps Co(8). One way to understand the structure is to inspect the Co(3)-, Co(8)-, Co(9)-, Si(3)-, and Si(6)-based polyhedra which interpenetrate into each other (Figure 1). The Si-based framework, shown in Figure 2, is composed of alternating Si(3)- and Si(6)-centered slabs along the *a* axis. To simplify the description and obtain a better view of the structure, only the bonds between the center atoms (Si(3) and Si(6)) and the surrounding atoms are shown. On a local scale, two types of structural fragments are noteworthy. In the first fragment, the Si(3) atom is bonded to another Si(3) atom forming a Si dimer (Figure 3A), with the Si(3)−Si(3) bond distance of 2.528(2) Å. Although this Si−Si bond distance is longer than the sum of the metallic radii of silicon, it is comparable to those in other intermetallics (2.523 Å in $Re_{24}Al_{102}Si_{12}$,[16] 2.518 Å in $FeAl_2Si$[17]). These two Si(3) atoms, together with two Co(9) atoms, form a Co_2Si_2 rhombus. This rhombus is surrounded by Al atoms with some serving to bridge the Si and Co atoms (Al(5), Al(7), Al(9), Al(12), and Al(17)), while others serving as links to the rest of the structure, Figure 3A. Similar Co_2Si_2 rhombic units are also found in other cobalt silicides such as $CoSi_2$, in which the Si−Si bond distance is 2.682 Å.[18]

Figure 3B depicts the Si(6)-centered polyhedra which conjoin in similar but not identical fashion to Si(3). In this fragment, two Si(6) and two Co(6) atoms also form a Co_2Si_2 rhombus; however, no Si−Si bonding exits with a Si(6)−Si(6) distance at 3.929 Å. The Si(6)-based dimeric polyhedra are linked to each other by bridging Co(8) atoms; when viewed down the *a* axis, these Si(6)-centered polyhedra form infinite puckered layers, Figure 3C.

The overall organization of the structure of $Co_{19}Al_{45}Si_{10-x}$ ($x = 0.13$) can be described as layers defined by Co(3), Co(8), and Co(9) polyhedra, which are linked to each other with a Si(3)- and Si(6)-based framework, Figure 4. The slabs composed of Co(3), Co(8), and Co(9) polyhedra, when viewed down the [001] direction, stack in A−A′ fashion where layer A′ is shifted relative to layer A along the *a* direction by *a*/2 (Figure 5). The center of the layer is occupied by Co(9) polyhedra forming a chain by vertex-linking. Both ends of the layer are capped by Co(3) and Co(8) polyhedra alternatively. As seen in Figure 6A, the connectivity mode of Co(9) polyhedra is very similar to that of Si(6):

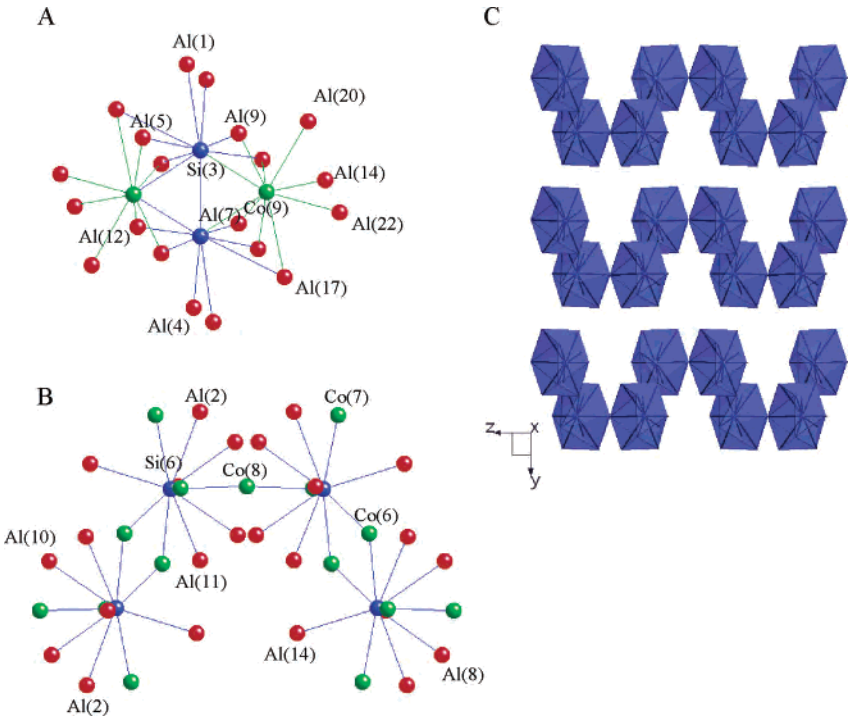

Figure 3. Structure of $Co_{19}Al_{45}Si_{10-x}$ ($x = 0.13$). (A) Coordination environment and local structure of two Si(3)-centered polyhedra joined via bridging Co(9) atoms to form a dimer. Si(3)−Si(3) distance: 2.5278 (21) Å. (B) The connectivity mode of Si(6)-centered dimers. (C) Extended organization of Si(6)-centered polyhedra forming a strongly correlated layer.

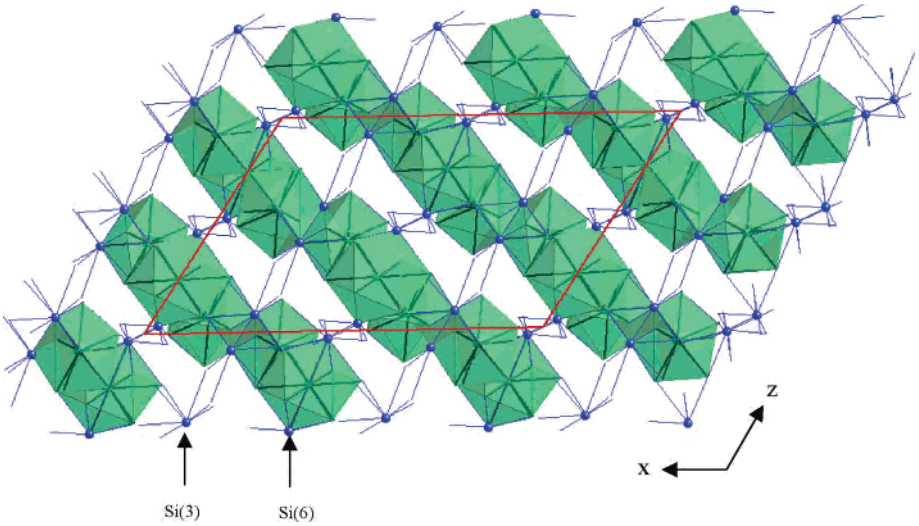

Figure 4. Structure of $Co_{19}Al_{45}Si_{10-x}$ ($x = 0.13$): the polyhedral view of Co(3), Co(8), and Co(9) atoms connected by Si-based wire framework.

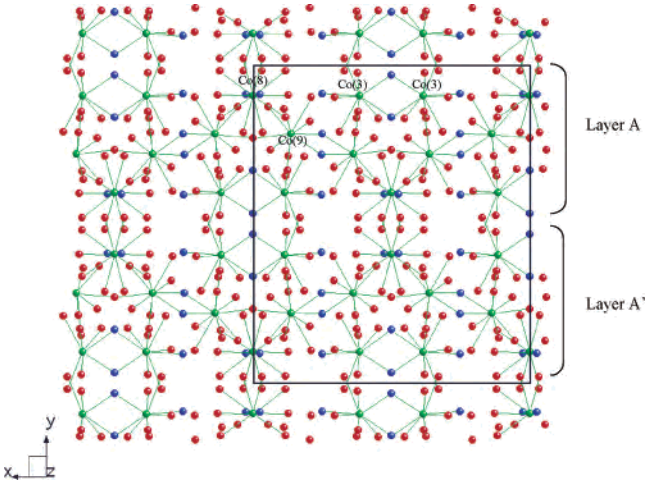

Figure 5. Structure of $Co_{19}Al_{45}Si_{10-x}$ ($x = 0.13$): the layered substructure of Co(3)-, Co(8)-, and Co(9)-based coordination polyhedra viewed in ball-and-stick representation down the *c* axis.

the Co_2Si_2 rhombic units, composed of two Co(9) and Si(3) atoms, are connected by bridging Al(20) atoms. Two Co(3) polyhedra are conjoined by bridging Si(2) and Si(4) atoms, forming a Co_2Si_2 rhombus, Figure 6B. Each Co(8) atom is sitting on a site of icosahedral geometry which contains two Si(6), Al(8), Al(10), Al(11), Al(23), and Al(2) atoms.

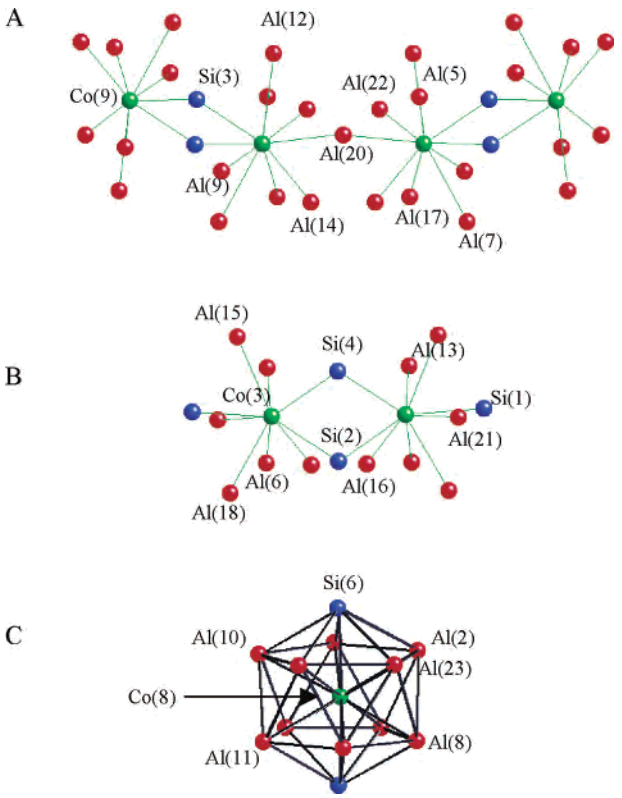

Figure 6. Structure of $Co_{19}Al_{45}Si_{10-x}$ ($x = 0.13$). (A) The connectivity mode of Co(9)-centered clusters. (B) The connectivity mode of Co(3)-centered polyhedra. (C) The coordination environment of Co(8) atom.

Crystal Structure of $Co_5Al_{14}Si_2$. $Co_5Al_{14}Si_2$ has a different structure type which appears to be new and is as highly elaborate as that of $Co_{19}Al_{45}Si_{10-x}$ ($x = 0.13$). This compound adopts the orthorhombic space group *Pnma*, which has 6 Co, 3 Si, and 15 Al independent atomic sites with a total of 168 atoms in the unit cell. Although $Co_{19}Al_{45}Si_{10-x}$ ($x = 0.13$) and $Co_5Al_{14}Si_2$ exhibit totally different structure types, they show notable similarities in the way the various polyhedra connect with each other. Both structural frameworks derive from the vertex-linkage of polyhedra with the Co_2Si_2 rhombus as the common feature in these structures.

(12) *Saint, Version 4*; Simens Analytical X-ray Instruments, Inc.: Madison, WI.
(13) Sheldrick, G. M. *SADABS*; University of Göttingen: Göttingen, Germany.
(14) Sheldrick, G. M. *SHELXTL, Structure Determination Programs, Version 5.0*; Siemens Analytical X-ray Instruments, Inc.: Madison, WI, 1995.
(15) To prepare $Co_{19}Al_{45}Si_{10-x}$ only from Co, Al, and Si, we tried the Al flux method and arc-melting. After arc-melting, we annealed the sample at 1000 °C for 3days. With both methods, the total reaction time was less than 6 d. We did not try the reactions as described in ref 10, which first includes arc-melting of the components, then annealing at 800 °C for 4 weeks. We believe the long annealing time at high temperature is necessary for form $Co_{19}Al_{45}Si_{10}$.
(16) Onogi, T.; Takeuchi, T.; Sato, H.; Mizutani, U. *J. Alloys Compd.* **2002**, *342*, 397.
(17) Geman, N. V.; Zavodnik, V. E.; Yanson, T. I.; Zarechnyuk, O. S. *Kristallografiya* **1989**, *34*, 738.
(18) Bertaut, F.; Blum, P. *Monatsh. Chem.* **1961**, *92*, 961.

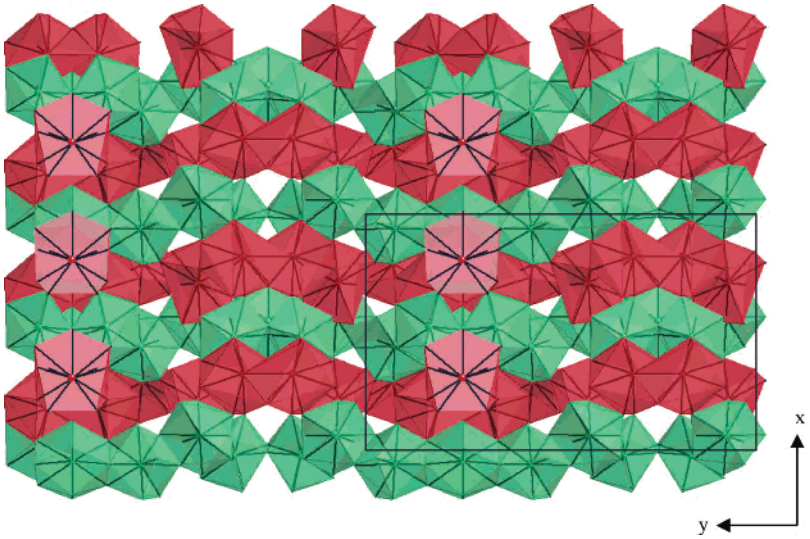

Figure 7. Structure of $Co_5Al_{14}Si_2$ in polyhedral representation down the *c* axis. Co, green; Al, red; Si, blue.

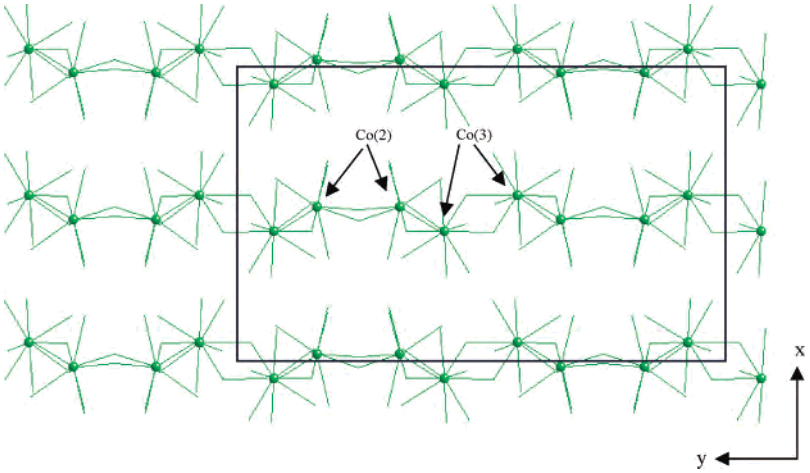

Figure 8. Partial structure of $Co_5Al_{14}Si_2$: the layered substructure of Co(2) and Co(3) polyhedra along the *a* axis.

Figure 7 depicts this structure in polyhedra of Al(1), Al(11), Al(15), Co(2), Co(3), and Co(5) atoms. One layer is based on Co polyhedra, and the second is based on Al polyhedra. To have a clearer view of the layered structural character of $Co_5Al_{14}Si_2$, only a ball-and-stick representation of the Co(2) and Co(3) polyhedra is shown in Figure 8. This figure shows dimeric units linked to each other by sharing Al(4), Al(9), and Al(12) atoms along the *b* direction. The local structure around these units is shown in Figure 9A and B. The manner in which the Co clusters connect with each other is very similar: two Co(2) polyhedra are connected by Si(3) and Al(6) atoms, while two Co(3) polyhedra are bridged by two Si(2) atoms. Such linking patterns show a resemblance to those of the Co(3) and Co(9) atoms formed in the structure of $Co_{19}Al_{45}Si_{10-x}$ ($x = 0.13$), which is an indication of the close structural relations of these two phases. Co(5) atoms, shown in Figure 9C, link the Co(2)-based dimers to form a "ribbon" running along the *c* axis, using one Al(6) and two Al(12) atoms as bridges.

The Al-based layer is shown in Figure 10. Interestingly, Al(11) and Al(15)-based polyhedra (ball-and-stick representation) form a similar layered structure as Co(2) and Co(3). As shown in Figure 11A, Al(15) polyhedra are linked by Al(5) atoms to form zigzag chains along the *c* axis. The Al(11) polyhedra are condensed into dimers by Al(11)−Al(11) bonding (distance 2.9280(24) Å) with Co(6) atoms acting as bridging atoms, Figure 11B. This unit is surrounded by more Al atoms to form a cluster. Furthermore, Al(1) polyhedra are connected to this cluster to form a larger trimer-based cluster, Figure 11C.

The local coordination geometries of Co(3), Co(8), and Co(10) in $Co_{19}Al_{45}Si_{10-x}$ ($x = 0.13$) and Co(2), Co(3), and Al(11) in $Co_5Al_{14}Si_2$ are presented in Figure 12A and B. As we can see, the Co atoms are surrounded by cages composed of Al and Si atoms. Such disposition is common in a variety of Al/Ga-rich binaries such as V_8Ga_{41},[19] WAl_{12},[20] and Co_2Al_9,[21] which also exhibit large and complex structures. Compared to another ternary intermetallic $Co_4Al_{7+x}Si_{2-x}$,[9] the only significant connection with the title compounds is the trigonal prismatic coordination geometry of Co atoms.

(19) Girgis, K.; Petter, W.; Pupp, G. *Acta Crystallogr. B* **1975**, *B31*, 113.
(20) Adam, J.; Rich, J. B. *Acta Crystallogr.* **1954**, *7*, 813.
(21) Bostroem, M.; Rosner, H.; Prots, Y.; Burkhardt, U.; Grin, Yu. Z. *Anorg. Allg. Chem.* **2005**, *631*, 534.

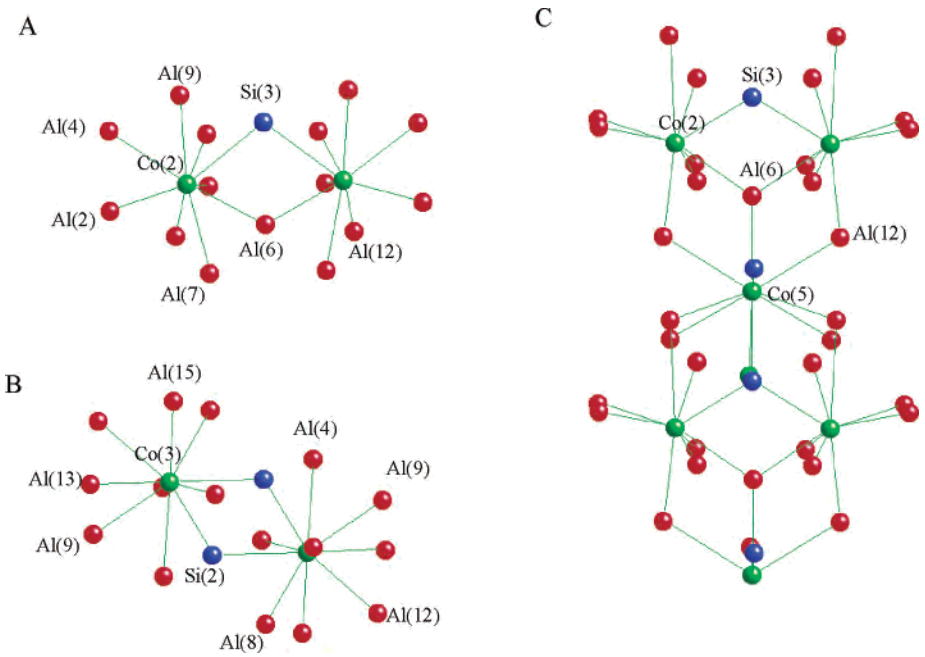

Figure 9. (A) Structure of the Co(2)-based dimeric fragment. (B) Structure of the Co(3)-based dimeric fragment. (C) The connectivity mode of Co(2) and Co(5) polyhedra along the *c* axis.

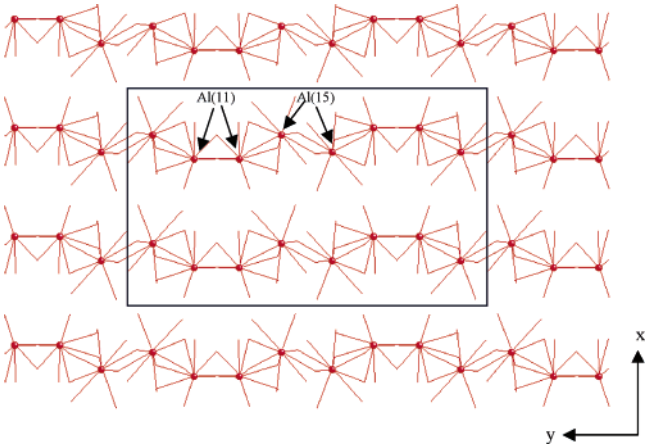

Figure 10. Layered substructure of Al(11) and Al(15) polyhedra in $Co_5Al_{14}Si_2$ along the *a* axis.

Another interesting feature about the structure of $Co_{19}Al_{45}Si_{10-x}$ and $Co_5Al_{14}Si_2$ is that, although there is no obvious evidence showing that they are approximants themselves, they show structural features that are reminiscent to some known quasicrystal approximants. For example, Figure 12C shows the first-neighbor coordination polyhedra of transition metals in the Mackay-type approximants $MnAl_6$,[22] α-FeAlSi,[23] and *o*-Co_4Al_{13}.[24] It is evident that, for most polyhedra in the structure of $Co_{19}Al_{45}Si_{10-x}$ and $Co_5Al_{14}Si_2$, we can find corresponding ones in the approximants, except that they are very distorted from ideal. In this sense, we might be able to consider these two phases as distorted Mackay-type approximants.

Physicochemical Properties. A noteworthy property of $Co_5Al_{14}Si_2$ is its inertness to thermal attack. When crystals of this compound were exposed to air in a thermal gravimetric furnace environment, there was no obvious ignition point, and up to 900 °C, only about 3% of weight gain was observed (Figure 13A). To further investigate the oxidation-resistance properties of this material, single crystals of $Co_5Al_{14}Si_2$ were loaded into an alumina crucible and annealed in air at 1000 °C for 5 h. The shiny and clean surface of the crystals was covered by an oxide layer which was observed by comparing the SEM images of $Co_5Al_{14}Si_2$ before and after annealing (Figure 13B−D). Elemental analysis by energy dispersive spectroscopy showed highly elevated levels of Al on the surface of the air-annealed crystals and the amount of Co and Si was less than 3%. This indicates that Al diffuses outward and reacts with oxygen on the surface of the material to form Al_2O_3, which is not spallable and blocks further oxygen transport into the material.

In contrast to $Co_5Al_{14}Si_2$ the compound $Co_{19}Al_{45}Si_{10-x}$ behaved very differently under the same conditions. Namely, up to 900 °C, this material showed weight gain of ∼10% much higher than that of $Co_5Al_{14}Si_2$. At higher temperatures, the oxidation accelerates leading to the oxides. EDS analysis on the surface of the crystals also show high amount of Al (above 50%) with the percentage of Co and Si at 2−3%. It is difficult to explain the difference in oxidation resistance between the two compounds from a structural point view; one reason might be that $Co_5Al_{14}Si_2$ has higher percentage of Al which could help to raise the oxidation resistance of the material by creating a better adhering Al_2O coating.

Aluminide intermetallics tend to preferentially form Al_2O_3 on their surfaces, such as in the case of NiAl and TiAl.[25] It has also been reported that addition of Al into $ZrSi_2$ and $MoSi_2$ helps to improve oxidation-resistance by forming a

(22) Stenberg, L.; Sjövall, R.; Lidin, S. *J. Solid State Chem.* **1996**, *124*, 65.
(23) Corby, R. N.; Black, P. J. *Acta Crystallogr. B* **1977**, *33*, 3468.
(24) Grin, J.; Burkhardt, U.; Ellner, M.; Peters, K. *J. Alloy Compd.* **1994**, *206*, 243.

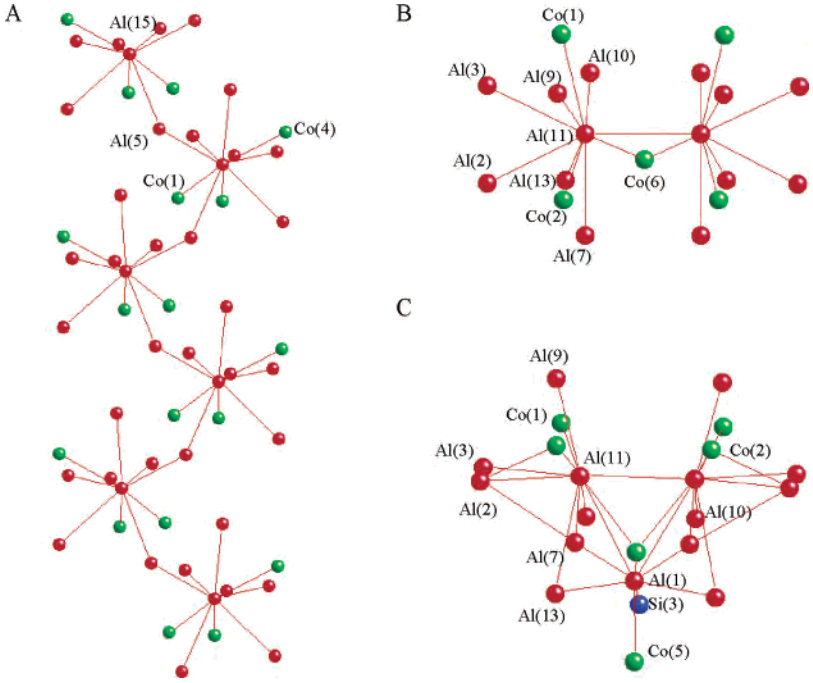

Figure 11. (A) Linkage of Al(15)-based polyhedra along the *c* axis. (B) Structure of the Al(11)-based dimer. (C) The fragment composed of Al(1) and Al(11) dimer.

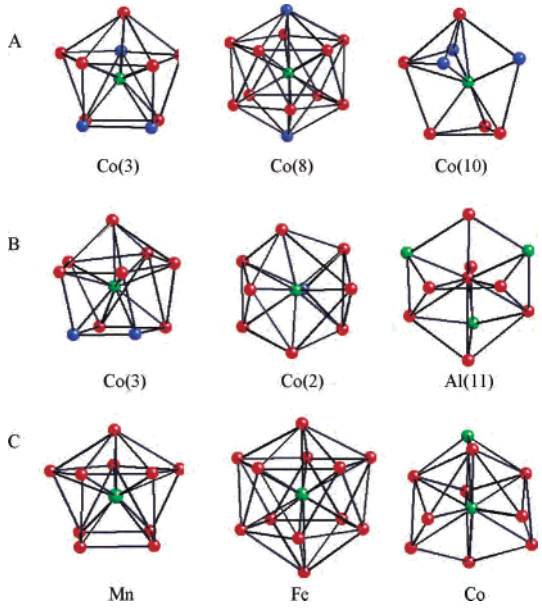

Figure 12. Coordination environments of (A) Co(3), Co(8), and Co(10) in $Co_{19}Al_{45}Si_{10-x}$ ($x = 0.13$). (B) Co(3), Co(2), and Al(11) in $Co_5Al_{14}Si_2$. (C) Selected transition metals in $MnAl_6$, α-FeAlSi, and *o*-Co_4Al_{13}.

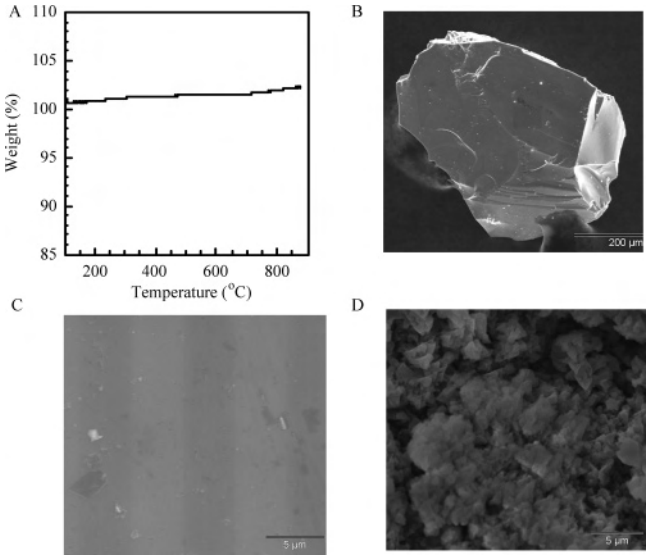

Figure 13. (A) Thermal gravimetric analysis of $Co_5Al_{14}Si_2$ in air. (B) Scanning electron micrograph of $Co_5Al_{14}Si_2$ before annealing. (C) (D) Close-up view of $Co_5Al_{14}Si_2$ before and after annealing at 1000 °C for 5 h.

protective Al_2O_3 layer.[26] However, the presence of Al_2O_3 was not detected by the X-ray diffraction analysis of the material after annealing probably because its very small amount. All observed Bragg peaks corresponded to the starting compound, which implies that the structural integrity of $Co_5Al_{14}Si_2$ was not compromised by annealing at 1000 °C. Similar thermal resistant properties have been found in $RE_5Co_4Si_{14}$ (RE = Ho, Er, Tm, and Yb), in which a protective SiO_2 layer was formed due to the Si-rich nature of the crystal framework.[27] The difference in the protecting layer between $Co_5Al_{14}Si_2$ and $RE_5Co_4Si_{14}$ suggest higher affinity of aluminum for oxygen than that of Co and Si. Although it has been observed that additions of Si to some aluminide alloys such as Ti_3Al result in a considerable reduction in the oxidation rate,[28] it cannot be the reason $Co_5Al_{14}Si_2$ shows better thermal properties than $Co_{19}Al_{45}Si_{10-x}$ ($x = 0.13$), since in $Co_5Al_{14}Si_2$ the Si atomic fraction is lower.

Magnetic susceptibility measurements showed that both compounds exhibit ferromagnetic behavior with $T_c \approx 260$

(25) Grabke, H. J. *Mater. Sci. Forum* **1997**, *251−254*, 149.
(26) Perez, P.; Lopez, M. F.; Jimenez, J. A.; Adeva, P. *Intermetallics* **2000**, *8*, 1393.
(27) Salvador, J. R.; Malliakas, C.; Gour, J. R.; Kanatzidis, M. G. *Chem. Mater.* **2005**, *17*, 1636.
(28) Jazayeri-G, A.; Buckley, R. A.; Davies, H. A. *Mater. Sci. Technol.* **2002**, *18*, 1485.

K; however, very low χ_m values were obtained ($\sim$0.015 emu/mol formula at 5 K). In addition, although the magnetization determined at 5 K showed hysteresis, the low-saturation magnetic moment (0.025 μ_B/mol formula at 10,000 Oe) indicates that the ferromagnetic behavior is likely caused by impurities. These may be nanocrystals of Co (unlikely given the very high Curie temperature of Co) or an unidentified compound occluded in the grains of single crystals.[29] We cannot exclude the fact that the pure bulk compounds may in fact be paramagnetic where the Co carries a small magnetic moment. Further work is needed to clarify this issue.

Concluding Remarks

The $Co_{19}Al_{45}Si_{10-x}$ ($x = 0.13$) and $Co_5Al_{14}Si_2$, grown from liquid Al, show exceptionally complex structures and large unit cells for ternary compounds. The extended structures can be described in terms of Co-, Al-, and Si-based substructures of distorted polyhedra of Co, Al, and Si atoms. The mild resemblance of the current structures to some quasicrystal approximants, especially in the first-neighbor coordination environments, may hint at the existence of quasicrystals in the ternary Co−Al−Si system. Preliminary evidence suggest that $Co_5Al_{14}Si_2$ is thermally oxidation resistant up to 1000 °C which may due to the formation of an Al_2O_3 layer on the surface of the crystals.

Acknowledgment. Financial support from the Department of Energy (Grant No. DE-FG02-99E45793) is gratefully acknowledged. This work made use of the SEM facilities of the Center for Electron Optics at Michigan State University.

Supporting Information Available: X-ray crystallographic data for the structure of $Co_{19}Al_{45}Si_{10-x}$ ($x = 0.13$) and $Co_5Al_{14}Si_2$ in the form of CIF files. This material is available free of charge via the Internet at http://pubs.acs.org.

IC052165K

(29) We could not however identify any distinct phases by SEM analysis or X-ray diffraction analysis.